

# Ganglioside accumulation in activated glia in the developing brain: comparison between WT and GalNAcT KO mice

Mariko Saito,<sup>1,\*†</sup> Gusheng Wu,<sup>§</sup> Maria Hui,<sup>\*</sup> Kurt Masiello,<sup>\*</sup> Kostantin Dobrenis,<sup>\*\*</sup> Robert W. Ledeen,<sup>§</sup> and Mitsuo Saito<sup>†,††</sup>

Divisions of Neurochemistry\* and Analytical Psychopharmacology,<sup>††</sup> Nathan S. Kline Institute for Psychiatric Research, Orangeburg, NY 10962; Department of Psychiatry,<sup>†</sup> New York University Langone Medical Center, New York, NY 10016; Department of Neurology and Neurosciences,<sup>§</sup> Rutgers-New Jersey Medical School, Newark, NJ 07103; and Dominick P. Purpura Department of Neuroscience,<sup>\*\*</sup> Rose F. Kennedy Center, Albert Einstein College of Medicine of Yeshiva University, Bronx, NY 10461

**Abstract** Our previous studies have shown accumulation of GM2 ganglioside during ethanol-induced neurodegeneration in the developing brain, and GM2 elevation has also been reported in other brain injuries and neurodegenerative diseases. Using GM2/GD2 synthase KO mice lacking GM2/GD2 and downstream gangliosides, the current study explored the significance of GM2 elevation in WT mice. Immunohistochemical studies indicated that ethanol-induced acute neurodegeneration in postnatal day 7 (P7) WT mice was associated with GM2 accumulation in the late endosomes/lysosomes of both phagocytic microglia and increased glial fibrillary acidic protein (GFAP)-positive astrocytes. However, in KO mice, although ethanol induced robust neurodegeneration and accumulation of GD3 and GM3 in the late endosomes/lysosomes of phagocytic microglia, it did not increase the number of GFAP-positive astrocytes, and the accumulation of GD3/GM3 in astrocytes was minimal. Not only ethanol, but also DMSO, induced GM2 elevation in activated microglia and astrocytes along with neurodegeneration in P7 WT mice, while lipopolysaccharide, which did not induce significant neurodegeneration, caused GM2 accumulation mainly in lysosomes of activated astrocytes. Thus, GM2 elevation is associated with activation of microglia and astrocytes in the injured developing brain, and GM2, GD2, or other downstream gangliosides may regulate astroglial responses in ethanol-induced neurodegeneration.—Saito, M., G. Wu, M. Hui, K. Masiello, K. Dobrenis, R. W. Ledeen, and M. Saito. **Ganglioside accumulation in activated glia in the developing brain: comparison between WT and GalNAcT KO mice.** *J. Lipid Res.* 2015. 56: 1434–1448.

**Supplementary key words** brain lipids • ethanol • inflammation • GM2/GD2 synthase knockout mice • activated microglia • astrocyte • lipopolysaccharide • ceramide • triglycerides • wild-type mice

This work was supported by National Institutes of Health/National Institutes on Alcohol Abuse and Alcoholism Grant R01 AA015355 to M.S. The authors have no conflicts of interest to disclose.

Manuscript received 2 December 2014 and in revised form 8 June 2015.

Published, *JLR Papers in Press*, June 10, 2015  
DOI 10.1194/jlr.M056580

Binge-like ethanol exposure in neonatal rodents, equivalent to the third trimester of human fetuses, induces robust neurodegeneration (1, 2) associated with reactive gliosis (3), activation of microglia (4, 5), and elevation of pro- and anti-inflammatory cytokines (6), resulting in long-lasting physiological and neurobehavioral deficits (7–10). This animal model of fetal alcohol spectrum disorders has been often used to clarify mechanisms behind ethanol toxicity during the developmental period, when neurons are particularly vulnerable to environmental toxins (11).

We previously demonstrated that ethanol-induced apoptotic neurodegeneration and microglial activation in postnatal day 7 (P7) mice (12–14) are associated with increases in brain lipids: ceramide, TG, cholesterol ester (ChE), *N*-acetylphosphatidylethanolamine (NAPE) (15), and GM2 ganglioside (16). Specifically, enhanced formation of sphingolipids, such as ceramide and GM2, appears to be involved in ethanol-induced neuroapoptosis (16–18). Gangliosides (sialic acid-containing glycosphingolipids), which have many biological functions as antigens, mediators of cell adhesion, and modulators of signal transduction (19, 20), are particularly abundant in the nervous system. In the P7 brain exposed to ethanol, GM2 ganglioside, which is a minor ganglioside in the brain and contains a relatively simple oligosaccharide moiety, increased mainly in lysosomes/late endosomes of activated microglia, suggesting that GM2 may be derived from more complex gangliosides of degenerating neurons (16) engulfed by activated microglia (14). Increased GM2 by ethanol exposure is also

Abbreviations: CatD, cathepsin D; ChE, cholesterol ester; FJ, Fluoro-Jade C; FJ<sup>+</sup>, Fluoro-Jade C-positive; GalNAcT, GM2/GD2 synthase; GFAP, glial fibrillary acidic protein; GFAP<sup>+</sup>, glial fibrillary acidic protein-positive; HPTLC, high-performance TLC; LPS, lipopolysaccharide; NAPE, *N*-acetylphosphatidylethanolamine; P7, postnatal day 7; TLR4, Toll-like receptor 4.

<sup>†</sup>To whom correspondence should be addressed.  
e-mail: marsaito@nki.rfmh.org

Copyright © 2015 by the American Society for Biochemistry and Molecular Biology, Inc.

detected in mitochondria and lysosomes in neurons, and GM2, as well as GD3 ganglioside, enhances cytochrome c release from isolated mitochondria (16), suggesting that GM2 may be involved in mitochondria-mediated apoptosis, as indicated for GD3 in CD95/Fas-mediated apoptosis in lymphocytes (21).

It has been shown that while GM2 is normally a minor ganglioside in the nervous system, it is transiently elevated during a restricted period of brain development (22) and significantly elevated not only in the brain of GM2 gangliosidosis, but also in the brain of other lysosomal storage disorders such as Niemann-Pick C disease, mucopolipidosis IV, and mucopolysaccharidoses (23–30). In addition, accumulation of GM2 has been observed in neurodegenerative diseases such as Alzheimer disease (31–33) and Angelman-like syndrome (34), and in rodent acute brain injury models such as blast-induced mild traumatic brain injury (35) and a transient focal cerebral ischemia model (36). However, the mechanisms behind and the roles of accumulated GM2 have not been well elucidated.

In order to explore the possible involvement of accumulated GM2 in neurodegeneration and glial activation, the present study compared the effects of ethanol between WT mice and mice with a disrupted *B4galnt1* gene encoding for GM2/GD2 synthase (GalNAcT), which leads to depletion of GM2, GD2, and all downstream gangliosides (37, 38). We found that ethanol increased the number of glial fibrillary acidic protein-positive (GFAP<sup>+</sup>) astrocytes in WT mice, in which punctate immunostaining of GM2 was detected in addition to previously reported GM2 accumulation in neurons and activated microglia (16). In the GalNAcT KO mice, while ethanol still induced neurodegeneration and accumulation of GD3 and GM3 in activated microglia, the increase in GFAP<sup>+</sup> astrocytes was now abolished. We further found that not only ethanol, but also DMSO and lipopolysaccharide (LPS) treatments, induced GM2 accumulation in activated microglia and astrocytes in P7 WT mice. Thus GM2 accumulation appears to be linked to glial activation in the injured developing brain.

## MATERIALS AND METHODS

### Animals

C57BL/6By mice were maintained at the animal facility of the Nathan S. Kline Institute for Psychiatric Research. All procedures followed guidelines consistent with those developed by the National Institutes of Health and the Institutional Animal Care and Use Committee of Nathan S. Kline Institute. GalNAcT KO (37) and the WT mice (C57BL/6J background) were maintained and bred in the animal facility of Rutgers-New Jersey Medical School. Genotyping was done by Transnetyx (Cordova, TN) using tail tips.

### Experimental procedure

C57BL/6By, GalNAcT KO, and littermate WT mice were treated at P7 with an ethanol treatment paradigm that induces robust apoptotic neurodegeneration (12). Each mouse in a litter was assigned to the saline or ethanol group. The mice were injected subcutaneously with saline or ethanol (2.5 g/kg, 20%

solution in sterile saline) twice at 0 h and 2 h. DMSO (Sigma-Aldrich, St. Louis, MO) (5 ml/kg or 10 ml/kg) was injected intraperitoneally into P7 C57BL/6By mice according to a method that induces neurodegeneration in P7 mice (39). Two microliters of saline or LPS (Sigma-Aldrich; serotype, 0127:B8) (1 mg/kg) in saline were injected intracerebrally into P7 C57BL/6By mice according to a method that induces brain injury, including astrogliosis, in P5 rats (40). Mice were kept with dams until brains were removed and processed for lipid analyses and immunohistochemical studies. In KO mice and their littermate WT mice, right hemispheres were used for lipid analyses and the left hemispheres were fixed in fixation solution for immunohistochemistry. For C57BL/6By mice, perfusion fixation was carried out for immunohistochemistry. Four to ten animals (C57BL/6By, GalNAcT KO, and littermate WT mice) derived from four to six litters were used for each data point.

### Lipid analysis

Whole brains or hemispheres were freshly isolated 24 h after treatment with ethanol, DMSO, LPS, or saline and were immediately soaked in 20 vol of a mixture of methyl-tert-butyl ether and methanol (1:1, v/v) on ice and kept for 1 week at 4°C to extract total lipids. The total lipid extracts were partitioned according to the method of Matyash et al. (41). The lower aqueous-methanol phase containing gangliosides was evaporated to dryness, applied to high-performance TLC (HPTLC) plates, and developed with chloroform/methanol/0.25% KCl (5:4:1) (42). The plates including various concentrations of GM2 standards were stained with an orcinol reagent, scanned with the Odyssey infrared system (LI-COR Biosciences, Lincoln, NE), and analyzed by Multi Gauge ver.2.0 (Fujifilm USA Medical Systems, Stamford, CT). The concentration of each ganglioside (presented as nanograms per milligram wet weight of brain) was calculated using GM2 standards. The upper organic methyl-tert-butyl ether phase obtained by the partition described above was evaporated to dryness and separated into neutral and acidic lipids using DEAE-Sephadex columns as described (43). The neutral lipid fraction (containing ceramide, cholesterol, TG, ChE, etc.) and various concentrations of ceramide, TG, and ChE standards were applied on HPTLC plates and developed first with hexane/ethyl acetate/water/acetic acid (3:4:5:2) until the solvent front ascended to 4 cm from origin, second with hexane/methyl-tert-butyl ether/acetic acid (65:35:2) until 6.5 cm, and third with hexane/methyl-tert-butyl ether/acetic acid (98/2/1) until 9 cm above origin. The acidic lipid fraction (containing NAPE, phosphatidic acid, sulfatide, etc.) and various concentrations of NAPE were developed on HPTLC with acetone/benzene/acetic acid/water (20:30:4:1). After development plates were first dipped in 20% methanol and then stained in 0.0001% primuline as described (44). Then, fluorescent lipid bands were scanned with the Gel Logic molecular imaging system (Carestream Health, Rochester, NY), and the concentrations of ceramide, TG, ChE, and NAPE (presented as nanograms per milligram wet weight of brain) were calculated from the corresponding standard lipids using Carestream Molecular Imaging software.

### Immunohistochemistry

Twenty-four to 48 h after the first ethanol injection, C57BL/6By mice were perfusion-fixed, as described previously (13), and the brain hemispheres from GalNAcT KO and littermate WT mice were immediately fixed in 4% paraformaldehyde solution at 4°C overnight. The fixed brains or hemispheres were transferred to phosphate-buffered saline solution and kept at 4°C for 2–5 days until cutting 50  $\mu$ m-thick vibratome sections. The free-floating sections were immunostained using anti-GM2 antibody (a mouse

monoclonal antibody from hybridoma clone 10-11, provided by Dr. Kostantin Dobrenis), anti-GD3 antibody (Seikagaku Biobusiness, Tokyo, Japan), anti-GM3 antibody (Cosmo Bio, Carlsbad, CA), anti-cathepsin D (CatD) antibody (provided by Dr. Mohan Panaiyur, Nathan Kline Institute), anti-CD68 antibody (AbD Serotec, Bio-Rad, Hercules, CA), anti-Iba-1 antibody (Wako Chemicals, Richmond, VA), anti-GFAP antibody (Millipore, Temecula, CA), and/or anti-LAMP1 antibody (Cell Signaling Technology, Danvers, MA) by a dual immunofluorescence method as described previously (13). Fluoro-Jade C (FJ) (Millipore) staining was performed according to the manufacturer's instruction. The extent of neurodegeneration detected by FJ staining was quantified in the cingulate cortex. The number of FJ-positive (FJ<sup>+</sup>) cells in each area of interest and the area of the area of interest were measured using the Image-Pro software version 4.5 (MediaCybernetics, Silver Spring, MD). The boundary of the cingulate cortex was defined in accordance with (45). FJ appeared to stain not only irregular-shaped degenerating cell bodies, but also other structures such as fragmented axons and dendrites. For quantification, only the degenerating cell bodies were counted. Automatic cell counting after correction (splitting adjacent cells and excluding artifacts) gave similar results to those of manual counting. The extent of neurodegeneration was expressed as the number of FJ<sup>+</sup> cells per square millimeter in the cingulate cortex. For each brain, data from three consecutive sections (each 50  $\mu$ m thick) were averaged and four brains (from four different litters) per treatment group were analyzed. The density of GFAP<sup>+</sup> cells in layers IV/V of the primary somatosensory cortex forelimb/hindlimb region (S1FL/HL) defined in accordance with (45) were calculated as described above for FJ<sup>+</sup> cells, and expressed as the number of GFAP<sup>+</sup> cells per square millimeter. The percentage of GM2<sup>+</sup> cells among GFAP<sup>+</sup> or Iba-1<sup>+</sup> cells was determined by manual counts in layers IV/V of the primary somatosensory cortex forelimb/hindlimb region (S1FL/HL), as described above. The percentage of FJ<sup>+</sup> cells among Iba-1<sup>+</sup> cells was also determined in the same region in the same manner. For each

brain, data from four to five sections (each 50  $\mu$ m thick) were averaged and four brains per group were analyzed. Photomicrographs were taken using 4 $\times$ , 10 $\times$ , 20 $\times$ , 40 $\times$ , or 100 $\times$  objectives with a Nikon Eclipse TE2000 inverted microscope equipped with a DXM1200F digital camera.

## Statistics

Values in the figures and tables are expressed as mean  $\pm$  SEM obtained from 4 to 10 samples. Statistical analyses of the data were performed by two-tailed Student's *t*-test and one- or two-way ANOVA using the SPSS statistics 22.0 program. A *P* value of <0.05 was considered significant.

## RESULTS

### Ethanol-induced neurodegeneration in P7 mice accompanies GM2 accumulation in microglia which engulf degenerating neurons

We have reported previously that ethanol exposure in P7 mice, which induces widespread apoptotic neurodegeneration and microglial activation within a day (12–14), increases GM2 ganglioside mainly in lysosomes/late endosomes of activated microglia (16), which appear to engulf degenerating neurons (14). Neurodegeneration was detected by FJ staining in many brain areas, including layers IV/V of the primary somatosensory cortex and the cingulate/retrosplenial cortex 24 h after ethanol exposure in P7 mice (Fig. 1A). In these brain sections, morphologically activated microglia, which were immunopositive for both Iba-1 (specific to microglia/macrophages) and CD68 (enriched in phagocytes) (Fig. 1F), showed a distribution pattern

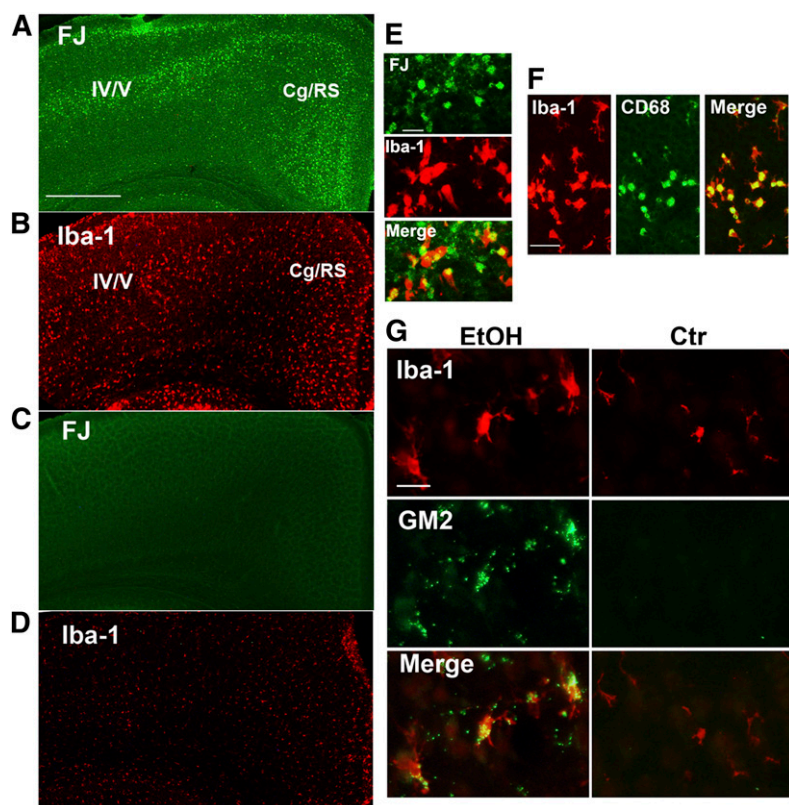


**Fig. 1.** Ethanol-induced neurodegeneration is associated with GM2 elevation in activated microglia. A: Twenty-four hours after ethanol exposure in P7 C57BL/6By mice, brains were removed and the sections were stained with FJ. A representative image shows the localization pattern of FJ<sup>+</sup> degenerating neurons in the cortex. Cg/RS, cingulate/retrosplenial cortex. Scale bar = 500  $\mu$ m. B: Brain sections prepared as described in (A) were immunolabeled with anti-Iba-1 antibody. A brain section adjacent to the one used for FJ staining shows that the distribution of morphologically activated microglia is similar to that of FJ<sup>+</sup> cells. On the other hand, FJ<sup>+</sup> cells were hardly detected in saline-treated control brain sections (C), and Iba-1<sup>+</sup> microglia with small cell bodies were evenly distributed (D). E: Brain sections prepared as described in (A) were dual-labeled with FJ and anti-Iba-1 antibody. FJ staining was frequently localized in activated microglia. Scale bar = 20  $\mu$ m. F: Brain sections prepared as described in (A) were dual-labeled with anti-Iba-1 antibody and anti-CD68 antibody. A representative image shows that microglia with an activated morphology were positive for both anti-Iba-1 and anti-CD68 immunolabeling. Scale bar = 50  $\mu$ m. G: Twenty-four hours after ethanol (EtOH) or saline (Ctr) exposure in P7 C57BL/6By mice, brains were removed and the sections were dual-labeled with anti-Iba-1 and anti-GM2 antibody. Activated microglia observed in ethanol-treated brain sections were positive for GM2, while GM2 immunostaining was hardly detected in the control brain. Scale bar = 20  $\mu$ m.



similar to that of degenerating neurons (Fig. 1B), although some of the Iba-1<sup>+</sup>CD68<sup>+</sup> cells could have been perivascular or invaded peripheral mononuclear macrophages. Dual labeling with FJ and anti-Iba-1 antibody showed that FJ staining was frequently localized in morphologically activated microglia (Fig. 1E), suggesting that degenerating neurons were phagocytosed by activated microglia. In the control (saline-treated) brain, FJ<sup>+</sup> cells were barely detected (Fig. 1C), and Iba-1<sup>+</sup> cells, which were mostly identified as resting microglia (Fig. 1G) except for amoeboid microglia in the corpus callosum (data not shown), were evenly distributed in the cortex (Fig. 1D). These activated microglia in the ethanol-treated brain generally displayed punctate anti-GM2 immunostaining, which was barely detectable in the control brain (Fig. 1G).

#### **Ethanol exposure in P7 mice increases GFAP<sup>+</sup> astrocytes that accumulate GM2 in late endosomes/lysosomes**

Time course studies (Fig. 2A) revealed that GM2 accumulation in activated microglia in layers IV/V of the primary somatosensory cortex shown in Fig. 1 (Area I in Fig. 2D) peaked 24 h after ethanol injection, but decreased 32 h after ethanol treatment, when punctate GM2 immunostaining was observed mainly in GFAP<sup>+</sup> cells with the morphology of astrocytes. Forty-eight hours after ethanol exposure, the majority of microglia showed morphology of resting microglia with no GM2 expression, while some astrocytes still remained GM2-positive. Figure 2B shows percentages of GM2<sup>+</sup>Iba-1<sup>+</sup> cells in total Iba-1<sup>+</sup> cells and percentages of GM2<sup>+</sup>GFAP<sup>+</sup> cells in total GFAP<sup>+</sup> cells, respectively. The cells were counted in Area I during the time course as described in the Materials and Methods. The punctate GM2 immunostaining found 32 h after ethanol exposure was frequently colocalized with LAMP1 and CatD immunolabeling (Fig. 2C), suggesting that GM2 accumulated in lysosomes/late phagosomes/late endosomes in astrocytes, as previously shown for activated microglia (16), because  $93 \pm 1.7\%$  (mean  $\pm$  SD of four animals) of GM2<sup>+</sup> punctate immunostaining was localized in GFAP<sup>+</sup> cells at this time point. The ethanol-induced staining for GM2 in astrocytes was observed not only in regions enriched in activated microglia/degenerating neurons, such as Area I, but also in the deep cortical layer/white matter near the cingulum and external capsule (Area II in Fig. 2D). Figure 2E shows such GM2 immunostaining in GFAP<sup>+</sup> cells in Area II. There were few degenerating neurons detected by FJ staining or morphologically activated microglia in Area II (Fig. 1A), although degenerating axons and dendrites have been detected in this region in our previous studies (14). Unlike Area I, where GM2 was mainly localized in activated microglia at 24 h after ethanol exposure (Fig. 2A),  $90 \pm 3.3\%$  (mean  $\pm$  SD from three animals) of the punctate GM2 immunostaining in Area II was found in astrocytes at 24 h. This GM2 staining in Area II also colocalized with CatD. In the control brain, GM2 staining was hardly detected, as previously reported (16), and the number of GFAP<sup>+</sup> astrocytes appeared less compared with that of ethanol-treated brain in both Areas I and II (Fig. 2D).

#### **Ethanol induces neurodegeneration and GD3/GM3 accumulation in activated microglia, but does not increase the number of astrocytes in GalNAcT KO mice**

In order to explore the mechanisms behind, and the significance of, GM2 accumulation in activated microglia and astrocytes, GalNAcT KO mice, which lack GM2, GD2, and downstream gangliosides, were injected with ethanol at P7 in the same manner as for the WT mice. Ethanol exposure in P7 KO mice induced neurodegeneration and microglial activation (Fig. 3A) similar to littermate WT mice and to C57BL/6By mice (Fig. 1), although the number of FJ<sup>+</sup> cells in the cingulate cortex, where neurodegeneration was robust, was significantly higher in ethanol-treated KO mice than in ethanol-treated WT mice 24 h after ethanol exposure (Fig. 3B, C). Here two-way ANOVA indicated that there was a highly significant main effect of genotype [WT versus KO;  $F(1,13) = 16.2$ ,  $P < 0.001$ ], in addition to the main effect of treatment [saline versus ethanol;  $F(1,13) = 177.3$ ,  $P < 0.001$ ]. Student's *t*-test also showed a significant difference ( $P = 0.0035$ ) between ethanol-treated WT and KO mice.

Ethanol-induced neurodegeneration in KO mice was accompanied by changes in lipid profiles. Table 1 shows the comparison of the effects of ethanol on brain lipid profiles between KO and WT mice. GD3, GM3, and 9-*O*-acetyl GD3 were major gangliosides in the KO brain because of the deletion of GalNAcT, as previously reported (37, 38, 46), and ethanol treatment further increased amounts of these gangliosides. We have shown previously not only GM2, but also other lipids, specifically ceramide, TG, ChE, and NAPE, increased in the ethanol-treated P7 mouse brain, and the elevation of these lipids appeared to be correlated with the severity of neural cell damage/death (15, 17). Our previous studies using cultured neurons (47) or P7 mice (15, 17) also suggest that the elevation of these lipids is partially due to enhanced lipogenesis and de novo ceramide synthesis by ethanol treatment. While we are not able to eliminate the possibility that ethanol increases the entry of serum lipids into the brain, our previous studies showing brain region-specific accumulation of TG, ChE, and NAPE (17), different accumulation kinetics among these lipids (15), and the different effects of neuroprotective agents on each lipid content (17, 48) suggest that the entry of serum lipids is not a major cause of the observed lipid elevation in the brain. Table 1 shows that ceramide, ChE, and NAPE also increased in KO mice treated with ethanol, although the elevation of TG did not reach a statistically significant level.

The cellular distribution of GD3 and GM3 in ethanol-treated KO mice was examined, as shown in Fig. 4. While low level diffuse immunostaining of GD3 and GM3 was detected throughout the control KO brain, ethanol treatment induced brighter aggregated or punctate staining for GD3 and GM3 mostly in activated microglia in Area I, while punctate GD3 or GM3 staining was hardly observed in Area II (the deep cortical layers/white matter area) (Fig. 4A, B). Ethanol also increased CatD levels in cells containing aggregated GD3 in Area I (Fig. 4C), which were mostly activated microglia (Fig. 4A, B). It appeared that the aggregated

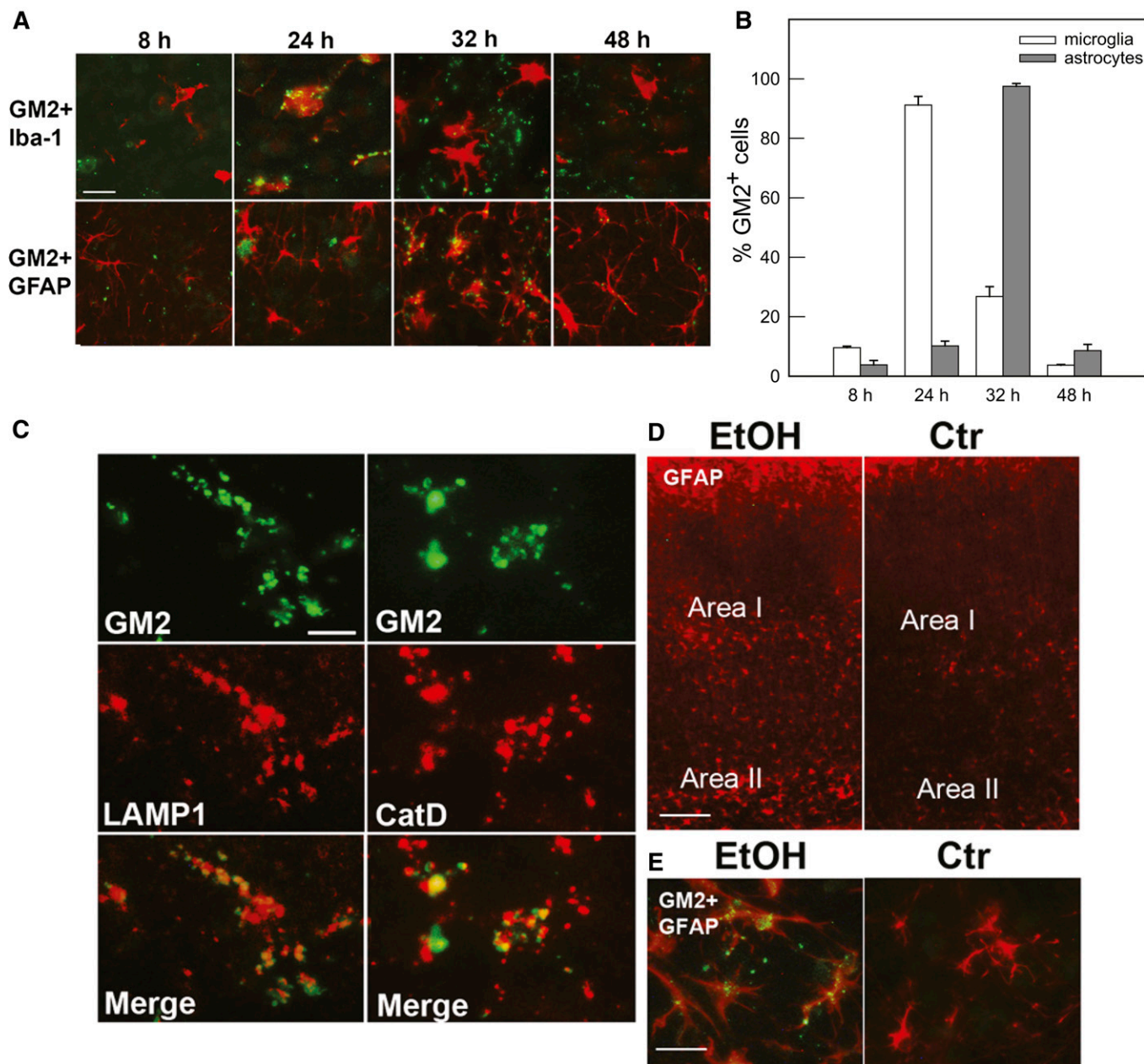


**Fig. 2.** Time course of GM2 expression in microglia and astrocytes, and colocalization of GM2 with LAMP1 and CatD in astrocytes. **A:** After ethanol exposure in P7 C57BL/6By mice (8, 24, 32, and 48 h), brains were removed and the sections were dual-labeled with anti-GM2 (green) and anti-Iba-1 (red) antibodies, or anti-GM2 (green) and anti-GFAP (red) antibodies. GM2, which was abundant in microglia 24 h after ethanol treatment, almost disappeared from these cells by 32 h, and GM2 was subsequently found in astrocytes. Scale bar = 20  $\mu$ m. **B:** The percentage of Iba-1<sup>+</sup> and GFAP<sup>+</sup> cells that were GM2<sup>+</sup> was determined in Area I [indicated in (D)] 8, 24, 32, and 48 h after ethanol exposure, as described in the Materials and Methods. **C:** Thirty-two hours after ethanol exposure in P7 C57BL/6By mice, brains were removed and the sections were dual-labeled with anti-GM2 and anti-LAMP1 antibodies, or anti-GM2 and anti-CatD antibodies. The images indicate partial colocalization of GM2 with LAMP1 and CatD, lysosomal markers. Scale bar = 5  $\mu$ m. **D:** Brain sections from P7 C57BL/6By mice perfusion-fixed 24 h after ethanol (EtOH) or saline (Ctr) exposure were immunostained with anti-GFAP antibody. The images show the cortex area: Area I corresponds to layers IV/V of the primary somatosensory cortex in Fig. 1A, and Area II corresponds to the deep cortical layer/white matter near the cingulum and external capsule. Ethanol treatment increased GFAP<sup>+</sup> astrocytes in Areas I and II. Scale bar = 100  $\mu$ m. **E:** Brain sections prepared as described in (D) were dual stained with anti-GM2 (green) and anti-GFAP (red) antibody. The images are taken from the Area II region and show evidence of GM2 in astrocytes. Scale bar = 20  $\mu$ m.

GD3 was partially colocalized with CatD, a lysosomal marker (Fig. 4C, D). The aggregated GD3 staining was not detected in either control or ethanol-treated WT brains, although light and diffuse GD3 staining was observed in neurons and glia of WT brains (data not shown). In order to examine further the possible accumulation of GD3/GM3 in the

degradation pathway in activated microglia, brain gangliosides were analyzed 24 or 48 h after P7 WT and KO mice were exposed to ethanol (Fig. 5A). In agreement with our previous studies (16), GM2 elevation induced by ethanol in the WT brain decreased greatly 48 h after the treatment. However, GM3 elevation in the KO mice remained high 48 h



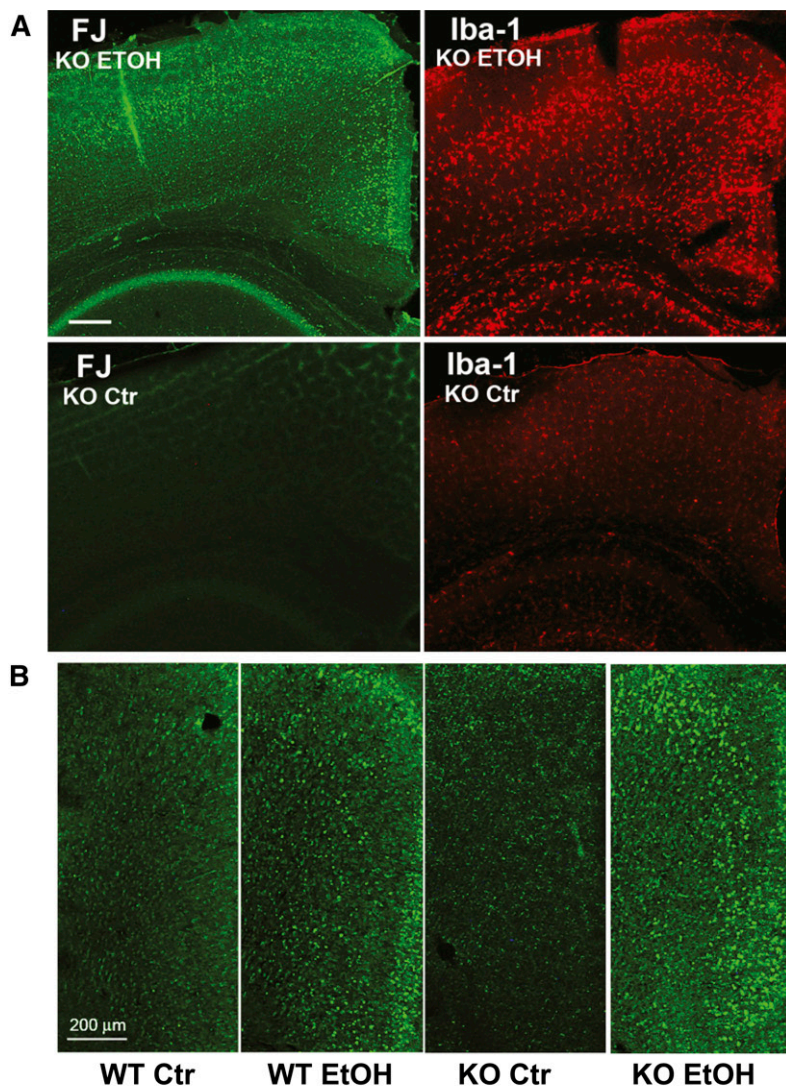
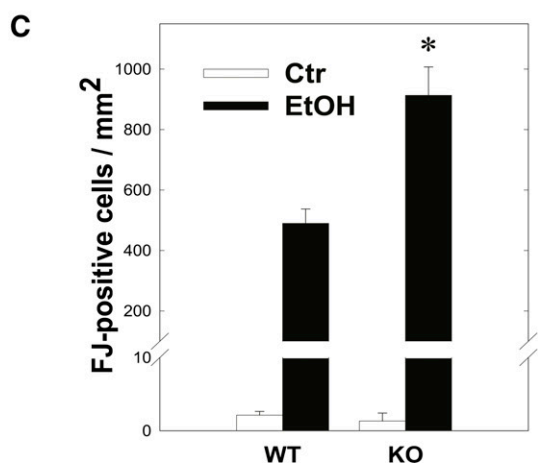


**Fig. 3.** Ethanol-induced neurodegeneration and microglial activation in GalNAcT KO mice. **A:** Twenty-four hours after P7 KO mice were treated with ethanol (EtOH) or saline (Ctr), brains were taken and the sections were stained with FJ or anti-Iba-1 antibody. Scale bar = 200  $\mu\text{m}$ . **B:** Twenty-four hours after P7 KO mice and littermate WT mice were treated with saline (Ctr) or ethanol (EtOH), brains were taken and the sections were stained with FJ. The images show the cingulate cortex area. Scale bar = 200  $\mu\text{m}$ . **C:** FJ<sup>+</sup> cells labeled as described above (B) were counted in the cingulate cortex, as described in the Materials and Methods. Two-way ANOVA indicated that there was a significant effect of genotype;  $F(1,13) = 16.2$ ,  $P < 0.001$ , and Student's *t*-test (\*) showed a significant difference ( $P = 0.0035$ ) between ethanol-treated WT and KO mice.



after ethanol exposure, although GD3 elevation was no longer detected. The accumulated GM3 observed 48 h after ethanol treatment was typically localized in microglia in layers IV/V of the S1 cortex (Fig. 5B). Also, the microglia in this region were frequently colabeled with FJ staining, and those FJ<sup>+</sup> microglia were much more abundant in KO mice than in WT mice 48 h after ethanol treatment (Fig. 5C, D). Thus, GM2 in the WT brain and GD3/GM3 in the KO

brain, which may be derived from degenerating neurons, were similarly accumulated in activated microglia, although clearance of these gangliosides appeared to be less efficient in KO mice. In contrast, the effects of ethanol on astrocyte activation and the ganglioside expression in astrocytes were clearly different between WT and KO mice. Twenty-four hours after ethanol injection, the number of GFAP<sup>+</sup> astrocytes increased in the WT brain (Fig. 6A, B) and GM2<sup>+</sup>

TABLE 1. The effects of ethanol on brain lipids in WT and GalNAcT KO mice

|          | WT           |                           | KO           |                           |
|----------|--------------|---------------------------|--------------|---------------------------|
|          | Ctrl         | EtOH                      | Ctrl         | EtOH                      |
| GM3      | 13.7 ± 2.4   | 19.4 ± 3.1                | 361.5 ± 47.3 | 629.5 ± 52.5 <sup>b</sup> |
| GM2      | 2.8 ± 1.4    | 18.4 ± 6.0 <sup>b</sup>   | n.d.         | n.d.                      |
| 9acGD3   | n.d.         | n.d.                      | 41.4 ± 0.8   | 46.3 ± 1.0 <sup>b</sup>   |
| GM1      | 107.7 ± 12.1 | 117.3 ± 23.5              | n.d.         | n.d.                      |
| GD3      | 26.1 ± 1.7   | 27.0 ± 5.3                | 698.7 ± 14.9 | 866.5 ± 48.8 <sup>b</sup> |
| GD1a     | 281.9 ± 15.8 | 273.1 ± 22.9              | n.d.         | n.d.                      |
| GD1b     | 9.1 ± 2.0    | 5.9 ± 1.2                 | n.d.         | n.d.                      |
| GT1b     | 21.4 ± 3.7   | 21.1 ± 0.9                | n.d.         | n.d.                      |
| Ceramide | 40.0 ± 5.5   | 60.3 ± 4.1 <sup>b</sup>   | 46.5 ± 5.4   | 69.8 ± 6.9 <sup>a</sup>   |
| NAPE     | 5.4 ± 1.5    | 90.4 ± 24.7 <sup>b</sup>  | 6.0 ± 1.8    | 131.9 ± 10.1 <sup>b</sup> |
| TG       | 289.3 ± 26.5 | 350.0 ± 25.7 <sup>a</sup> | 273.8 ± 28.3 | 325.5 ± 26.7              |
| ChE      | 12.3 ± 2.3   | 165.1 ± 12.0 <sup>b</sup> | 13.1 ± 3.5   | 209.2 ± 13.5 <sup>b</sup> |

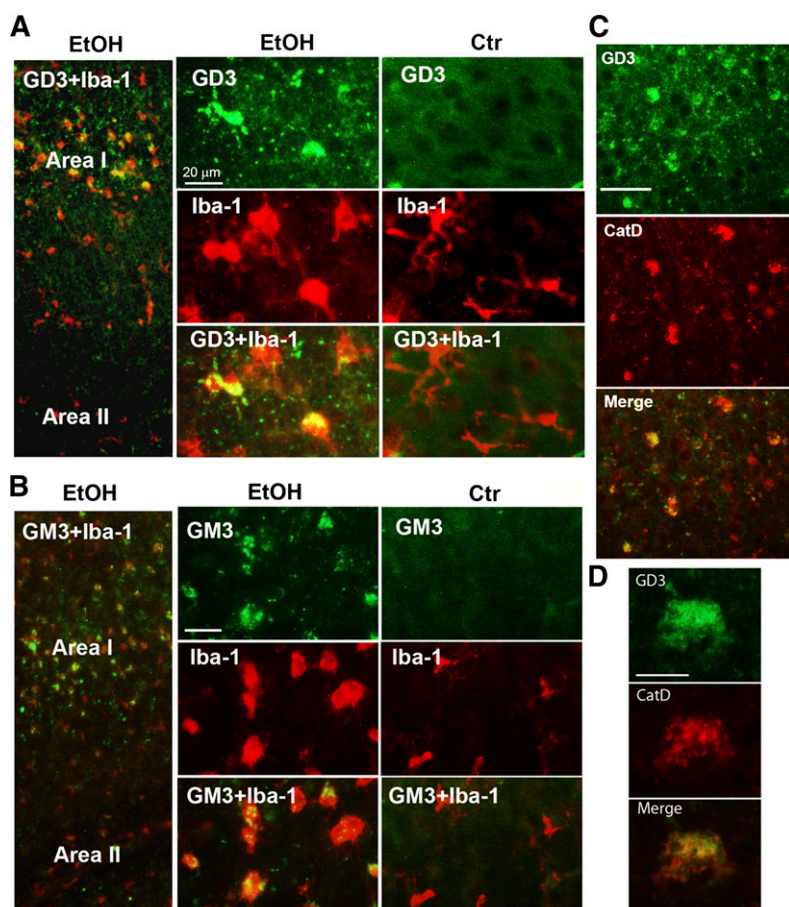
P7 WT and KO mice were exposed to saline (Ctrl) or ethanol (EtOH) at P7, and the amounts of gangliosides, ceramide, NAPE, TG, and ChE of the brain taken after 24 h were analyzed, as described in the Materials and Methods, and presented as nanograms per milligram wet weight of brain. Ganglioside nomenclature follows Svennerholm (79). 9acGD3, 9-*O*-acetyl GD3; n.d., not detected.

<sup>a</sup>*P* < 0.05, significantly different between the ethanol and control groups by Student's *t*-test.

<sup>b</sup>*P* < 0.01, significantly different between the ethanol and control groups by Student's *t*-test.

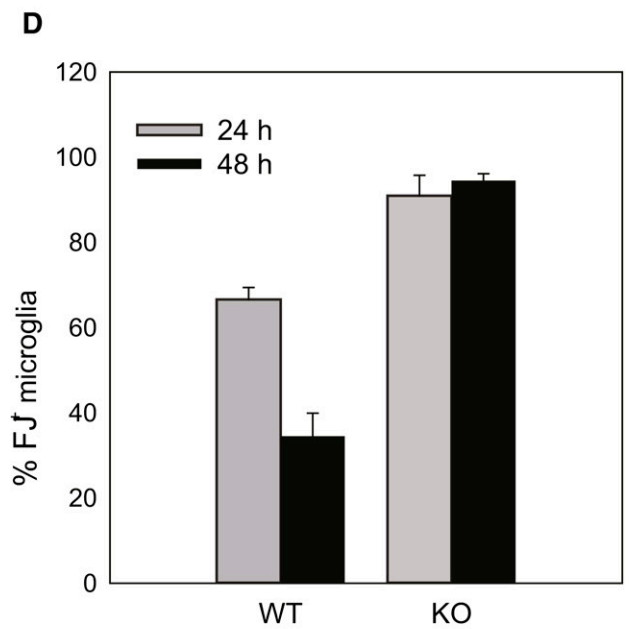
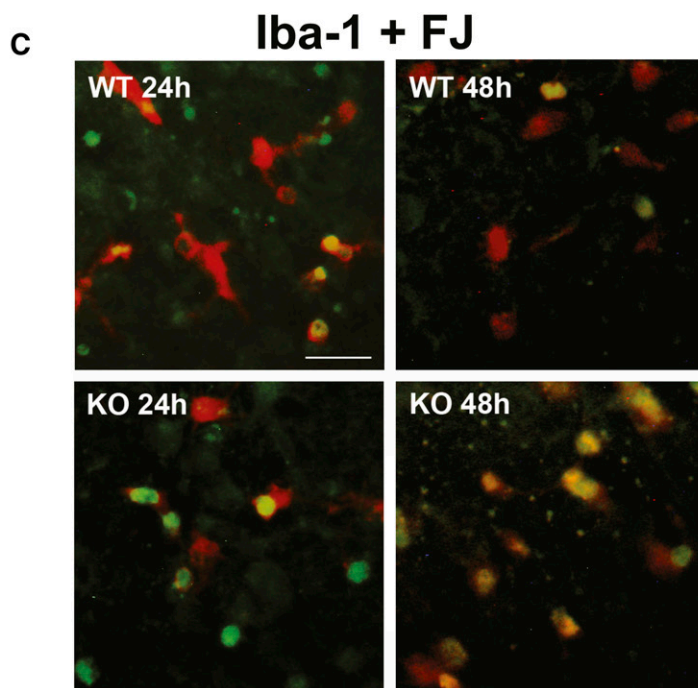
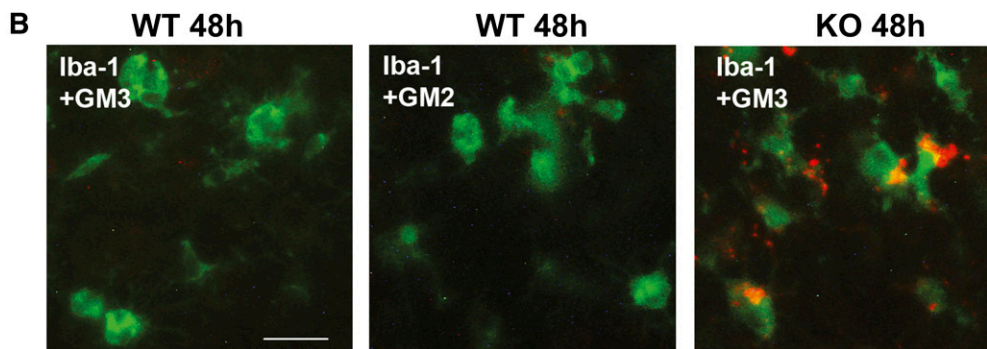
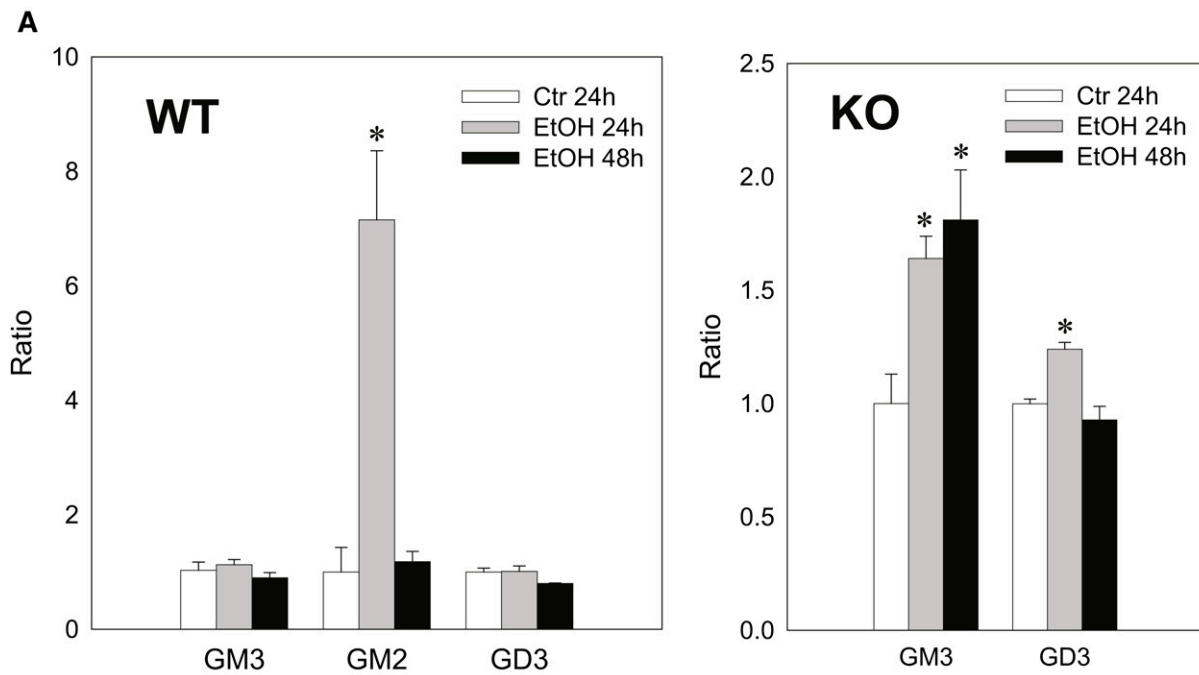
astrocytes were detected in Area II (Fig. 6A). However, while punctate GD3 or GM3 staining was sometimes observed in astrocytes in Area I, such GM3 or GD3 staining was rarely detected in Area II in the KO mice exposed to ethanol (Fig. 6C), and as shown in Fig. 4, GM3<sup>+</sup> as well as GD3<sup>+</sup> aggregates were mostly found in activated microglia in Area I. As expected, GM2 immunostaining was not detected in KO mice, further confirming the specificity of GM2 antibody

used in the present study (Fig. 6D). Because ethanol appeared to increase the number of GFAP<sup>+</sup> astrocytes (Fig. 6A, B) in the WT brain, we compared the number of GFAP<sup>+</sup> astrocytes in Area I, specifically in layers IV/V of the S1 cortex, 24 h after saline/ethanol exposure in P7 WT and KO mice (Fig. 7). ANOVA indicated that the main effect of treatment (saline/ethanol) was significant [*F*(1,12) = 16.8, *P* = 0.001]. However, there was a significant interaction



**Fig. 4.** Ethanol-induced aggregated or punctate immunostaining of GD3 and GM3 in activated microglia in the KO mice. A: Twenty-four hours after P7 KO mice were treated with ethanol (EtOH) or saline (Ctrl), brains were taken and the sections were dual-labeled using anti-GD3 (green) and anti-Iba-1 (red) antibody. Punctate or aggregated GD3, only observed in the ethanol-treated brain, was detected mainly in activated microglia. Scale bar = 20 μm. B: Under the same experimental conditions, punctate or aggregated GM3 was also found in activated microglia in ethanol-treated KO mice, while aggregated or punctate GM3 staining was rarely detected in control KO mice. Scale bar = 20 μm. C: Brain sections taken from KO mice 24 h after ethanol exposure were dual-labeled with anti-GD3 (green) and anti-CatD (red) antibody. Punctate or aggregated GD3 was frequently colocalized with CatD. Scale bar = 50 μm. D: A sample cell dual-labeled with anti-GD3 and anti-CatD antibody, as described in (C), examined with a higher magnification objective. Scale bar = 10 μm.







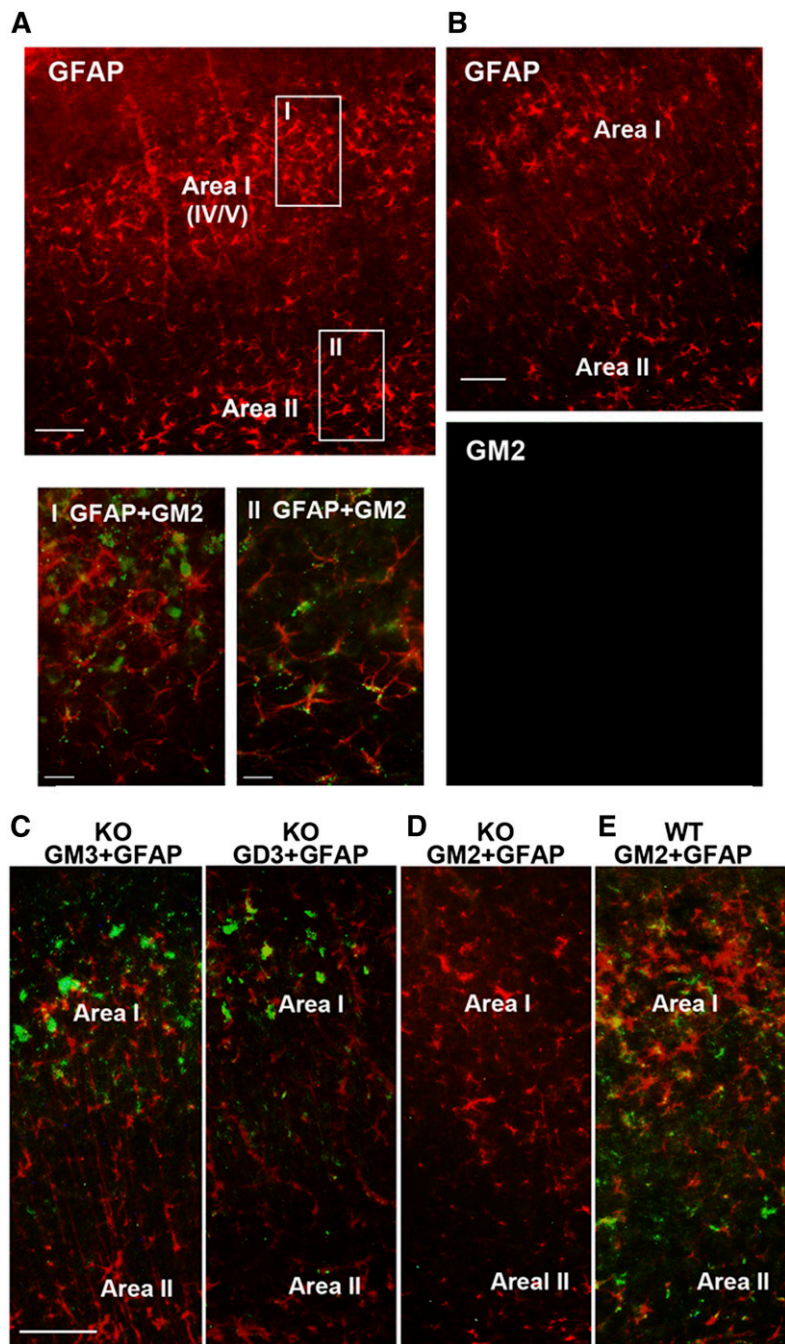


**Fig. 6.** The comparison of distribution of accumulated GM2 in WT mice and accumulated GM3/GD3 in KO mice. A: Twenty-four hours after WT mice were treated with ethanol, brains were taken and the sections were dual-labeled with anti-GFAP (red) and anti-GM2 (green) antibodies. Only GFAP staining is shown in the upper panel. Accumulation of GM2 was detected not only in Area I, where degenerating neurons were abundant, but also in Area II, where GM2 was localized in GFAP<sup>+</sup> astrocytes. The lower panels show the brain areas indicated as boxes I and II in the upper panel. The scale bar in the upper panel is 100  $\mu\text{m}$ , and 20  $\mu\text{m}$  in lower panels. B: Panels show examples of a brain section from control mice dual-labeled with anti-GFAP (upper) and anti-GM2 (lower) antibodies. GM2 was hardly detected in the control brain in both Area I and Area II. Scale bar = 100  $\mu\text{m}$ . C: Twenty-four hours after P7 KO mice were exposed to ethanol, brains were harvested and the sections were dual-labeled with anti-GFAP (red) antibody and anti-GM3 or anti-GD3 (green) antibody. GM3 and GD3 immunostaining was hardly detected in Area II. Scale bar = 100  $\mu\text{m}$ . D: Twenty-four hours after P7 KO mice were exposed to ethanol, brains were removed and the sections were dual-labeled with anti-GM2 (green) and anti-GFAP antibody (red). As expected, GM2 was not stained in KO mice. E: Twenty-four hours after P7 WT mice were exposed to ethanol, brains were removed and the sections were dual-labeled with anti-GM2 (green) and anti-GFAP (red) antibody. GM2 staining was detected in astrocytes in both Area I and Area II.

between genotype and treatment [ $F(1,12) = 17.8, P = 0.001$ ], and the number of GFAP<sup>+</sup> astrocytes significantly ( $P = 0.003$ , by Student's *t*-test) increased in WT mice exposed to ethanol, but not in KO mice. The increase in

GFAP<sup>+</sup> astrocytes in P7 WT mice treated with ethanol agreed with a previous study indicating that ethanol exposure in neonatal rats (between P4 and P10) increased GFAP expression in cortical layer V (3).

**Fig. 5.** Accumulation of GM3 and FJ staining in microglia 48 h after ethanol treatment. A: Twenty-four or 48 h after P7 WT and KO mice were exposed to saline/ethanol, brain gangliosides were analyzed, as described in the Materials and Methods. The amounts of gangliosides (GM3, GM2, and GD3) in WT or KO mice 48 h after ethanol exposure are expressed as ratios to the amounts of 24 h control (Ctr) samples. \* $P < 0.05$ , the value is significantly different from the 24 h control group by one-way ANOVA with Bonferroni's post hoc test. B: Forty-eight hours after P7 WT and KO mice were treated with ethanol, brains were taken, and the sections were dual-labeled with anti-Iba-1 (green) and anti-GM3 (red) or anti-GM2 (red) antibody. Many microglia are GM3<sup>+</sup> in layers IV/V of the S1 cortex in the KO brain. Scale bar = 20  $\mu\text{m}$ . C: Brain sections taken from WT and KO mice 24 or 48 h after ethanol exposure were dual-labeled with anti-Iba-1 (red) antibody and FJ (green) staining. Many microglia are FJ<sup>+</sup> in layers IV/V of the S1 cortex in KO mice 48 h after ethanol treatment. Scale bar = 20  $\mu\text{m}$ . D: The percentages of FJ<sup>+</sup> cells among Iba-1<sup>+</sup> cells in layers IV/V of the S1 cortex were calculated using images including those shown in (C). Two-way ANOVA indicated that there was a significant interaction between the effects of genotype (WT versus KO) and time (24 h versus 48 h) [ $F(1,17) = 18.4, P < 0.001$ ], a significant main effect of genotype [ $F(1,17) = 102.9, P < 0.001$ ], and a significant main effect of time [ $F(1,17) = 11.8, P = 0.003$ ].

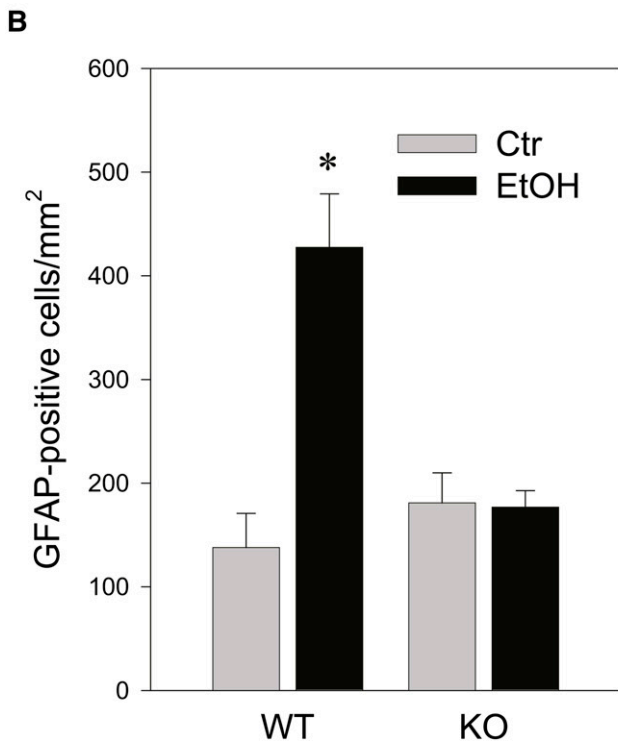
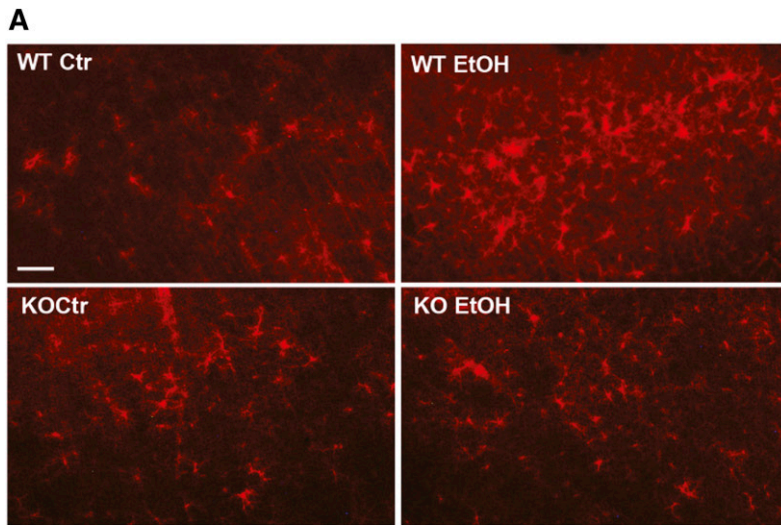


**Fig. 7.** The effects of ethanol on the number of GFAP<sup>+</sup> cells in WT and KO mice. **A:** Brains were harvested 24 h after WT and KO mice were exposed to saline (Ctr) or ethanol (EtOH) at P7, and brain sections were immunostained with anti-GFAP antibody. Scale bar = 100  $\mu$ m. **B:** The density of GFAP<sup>+</sup> cells in layers IV/V of the S1 cortex were calculated, as described in the Materials and Methods, using brain sections including those shown in (A).

#### GM2 elevation occurs in microglia and/or astrocytes of P7 mice treated with DMSO and LPS

The above results suggested that there may be a relationship between ethanol-induced GM2 elevation and glial activation. We then tested the possibility that treatments other than ethanol, which are known to induce neurodegeneration and/or glial activation, increase GM2 levels in the developing brain. It has been shown that DMSO, like ethanol, induces neurodegeneration in P7 mice (39). Therefore, lipid profiles of the brain harvested 24 h after the intraperitoneal injection of DMSO into P7 C57BL/6By mice were analyzed as described in the Materials and Methods. As shown in **Table 2**, elevation of GM2 was observed in the brain treated with 10 ml/kg of DMSO. This dose of DMSO has been shown to induce widespread caspase-3 activation in the P7 brain (39). In addition to the

increase in GM2, there were highly significant increases in NAPE and ChE, as observed in ethanol-induced neurodegeneration (Table 1) (15, 17). Immunohistochemical studies (**Fig. 8A, B**) revealed that punctate GM2 staining was localized in activated microglia and GFAP<sup>+</sup> astrocytes in Areas I and II in a manner similar to ethanol exposure. FJ<sup>+</sup> cells were also observed in the cingulate cortex region (**Fig. 8C**), although less robust in comparison with ethanol-treated samples. We also examined the effects of intracerebral injection of LPS on the brain of P7 C57BL/6By mice, using a method that induces glial activation in the early postnatal rat brain (40). As shown in **Table 3**, LPS induced significant increases in GM2, NAPE, and ChE, although these increases were less prominent compared with ethanol or DMSO treatment, and the ceramide levels were unchanged. These more modest changes may be



TABLE 2. The effects of DMSO on brain lipids in P7 C57BL/6By mice

|          | Ctrl       | DMSO 5                  | DMSO 10                  |
|----------|------------|-------------------------|--------------------------|
| GM2      | 2.7 ± 0.3  | 4.3 ± 0.9               | 23.6 ± 1.5 <sup>b</sup>  |
| Ceramide | 50.2 ± 1.8 | 64.2 ± 2.5 <sup>a</sup> | 74 ± 1.9 <sup>b</sup>    |
| NAPE     | 10 ± 0.7   | 11.7 ± 1.3              | 357 ± 92.3 <sup>b</sup>  |
| TG       | 320.6 ± 17 | 349.3 ± 6.7             | 373.3 ± 11.7             |
| ChE      | 38.3 ± 12  | 27.3 ± 9.6              | 181.7 ± 5.2 <sup>b</sup> |

Twenty-four hours after P7 C57BL/6By mice were exposed to 10 ml/kg of saline (Ctrl), 5 ml/kg of DMSO, or 10 ml/kg of DMSO, brains were taken, and the amounts of GM2, ceramide, NAPE, TG, and ChE were analyzed as described in the Materials and Methods, and presented as nanograms per milligram wet weight of brain.

<sup>a</sup>*P* < 0.05, the value is significantly different from the saline group by one-way ANOVA with Bonferroni's post hoc test.

<sup>b</sup>*P* < 0.001, the value is significantly different from the saline group by one-way ANOVA with Bonferroni's post hoc test.

related to the observation that degenerating neurons were hardly detected by FJ staining 24 h after LPS treatment (data not shown). However, LPS increased the number of GFAP<sup>+</sup> astrocytes (Fig. 9B) compared with the control (Fig. 9E) as reported in neonatal rats (40), and punctate GM2 immunostaining was frequently detected in astrocytes (Fig. 9C, D) in ipsilateral sites of the brain (Fig. 9F). These GFAP<sup>+</sup> astrocytes were more evenly distributed in the cortex than the ethanol-treated brain (Figs. 2D, 6A), and some of the punctate GM2 were colocalized with CatD (Fig. 9H), as observed in the ethanol-treated brain (Fig. 2C). In the LPS-treated brain, GM2 was barely detected in microglia (Fig. 9G), and morphologically activated microglia were scant and were not concentrated in Area I. Thus, GM2 accumulation occurred not only by ethanol

treatment, but also by other treatments known to induce neurodegeneration and glial activation.

## DISCUSSION

We have shown here that ethanol, DMSO, and LPS treatments, which induce acute neurodegeneration and/or glial activation in the P7 mouse brain, caused elevation of GM2 ganglioside in activated microglia and astrocytes, suggesting that GM2 elevation is associated with glial activation in the developing brain.

Our previous studies (16) have demonstrated that ethanol-induced neurodegeneration and the associated microglial activation in the neonatal brain are accompanied by GM2 accumulation in lysosomes/late phagosomes/late endosomes in activated microglia, which appear to engulf degenerating neurons (14). This notion was further supported by the present study, which indicated that microglia activated by ethanol were positive for CD68 (Fig. 1F), a presumed marker for phagocytic cells (49), and that FJ staining, that labeled degenerating neurons and their fragments, was often localized in these phagocytic microglia (Fig. 1E). The current study, using GalNAcT KO mice, showed that ethanol triggered robust neurodegeneration and surrounding microglial activation in these mice (Fig. 3), which were associated with accumulation of GD3 and GM3 (major gangliosides in the KO mice) in lysosomes of activated microglia (Fig. 4). The abundance of FJ-stained microglia in KO mice exposed to ethanol (Fig. 5C) indicates that microglia in these mice also phagocytosed degenerating neurons.

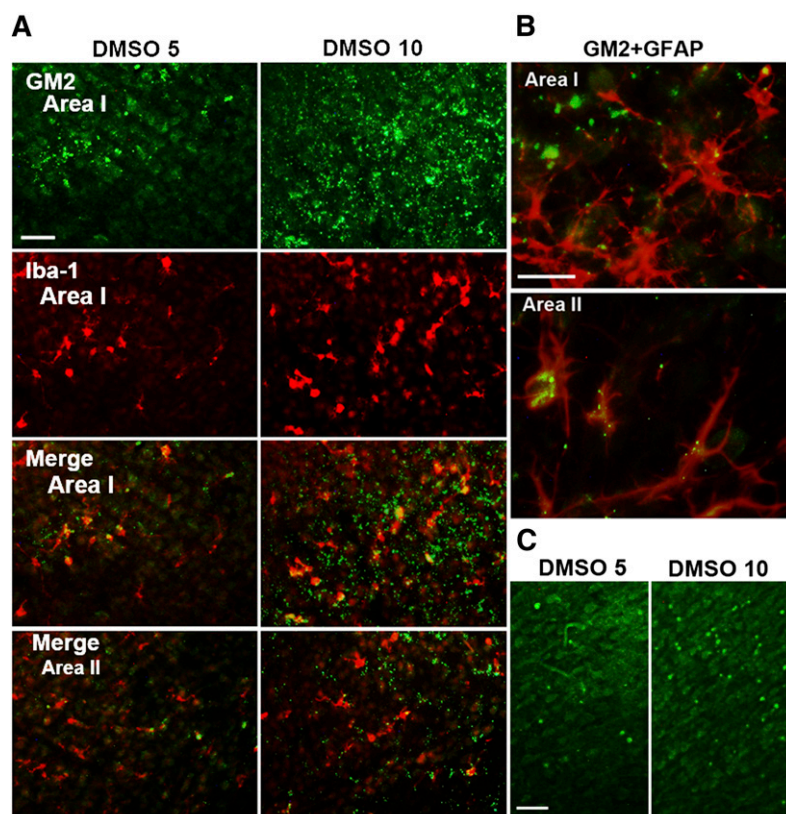


Fig. 8. GM2 accumulation in microglia and astrocytes in the brain of mice exposed to DMSO. A: P7 C57BL/6By mice were injected with DMSO (5 ml/kg or 10 ml/kg) intraperitoneally, and the brain was perfusion-fixed 24 h after the injection. Brain sections were dual-labeled with anti-GM2 (green) and anti-Iba-1 (red) antibody. GM2 was observed in most of the activated microglia in Area I. Scale bar = 50 μm. B: The sections from brains treated with 10 ml/kg of DMSO were dual-labeled with anti-GM2 (green) and anti-GFAP (red) antibody. GM2 was localized also in astrocytes, especially in Area II. Scale bar = 20 μm. C: The sections from brains treated with 5 or 10 ml/kg of DMSO were stained with FJ. The images show the cingulate cortex region. Scale bar = 50 μm.

TABLE 3. The effects of LPS injection on brain lipids in P7 C57BL/6By mice

|          | Ctrl        | LPS                     |
|----------|-------------|-------------------------|
| GM2      | 5.8 ± 1.4   | 9.8 ± 1.4 <sup>a</sup>  |
| Ceramide | 48.6 ± 1.7  | 47.1 ± 1.9              |
| NAPE     | 16.9 ± 2.2  | 38.8 ± 5.3 <sup>b</sup> |
| TG       | 236.9 ± 1.5 | 250 ± 14.9              |
| ChE      | 33.5 ± 3.8  | 51 ± 2.4 <sup>b</sup>   |

Twenty-four hours after P7 C57BL/6By mice were injected with saline (Ctrl) or LPS (1 mg/kg), brains were taken, and the amounts of GM2, ceramide, NAPE, TG, and ChE were analyzed as described in the Materials and Methods, and presented as nanograms per milligram wet weight of brain.

<sup>a</sup> $P < 0.05$ , the value is significantly different between the saline and the LPS groups by Student's *t*-test.

<sup>b</sup> $P < 0.01$ , the value is significantly different between the saline and the LPS groups by Student's *t*-test.

Accumulated gangliosides (GM2 in WT mice and GM3/GD3 in KO mice) in activated microglia may be derived from overloaded gangliosides of degenerating neurons engulfed by microglia, based on the subcellular localization of accumulated gangliosides. Especially, accumulation of GM3, but not GD3, in the KO mice 48 h after ethanol treatment (Fig. 5A, B) indicates that ganglioside accumulation occurs in the degradation pathway. Compared with the accumulation of GM2 in WT mice, the amounts of GD3/GM3 increased in the KO mice by ethanol were much higher (Table 1). The apparent slower clearance of accumulated gangliosides and FJ<sup>+</sup> debris in KO mice compared with that of WT mice (Fig. 5) may suggest that the endosomal/

lysosomal degradation pathway is more disturbed in the KO mice. The KO mice may need to eliminate a higher number of degenerating neurons than WT mice, or the endosomal/lysosomal pathway may be disrupted in the KO mice because of the lack of GM2/GD2 or downstream gangliosides. In addition, the accumulation of GM2 or GD3/GM3 may be promoted by enhanced lipogenesis and augmented de novo ceramide/ganglioside synthesis by ethanol, as we have shown previously in C57BL/6By mice (15, 17) and in cultured neurons (47). While mechanisms of preferential elevation of GM2 in phagocytic microglia in WT mice remain to be elucidated, accumulation of simple gangliosides, such as GM3 and GM2, have often been reported in lysosomal storage diseases, neurodegenerative diseases, and neuroinjury models (23, 27–29, 34–36, 50, 51). Even when a primary deficiency in a lysosomal glycohydrolase, activator protein, or saposin directly involved in the degradation of GM2 or GM3 (52) is not present, the accumulation of GM2/GM3 appears to occur, at least in part, in the endosomal/lysosomal system (26, 29, 30, 34, 53) and/or in lipid rafts (24, 27, 33). As well as for deficiencies in catabolic proteins not directly involved in degradation of these gangliosides, defects in trafficking of gangliosides from endosomes to the Golgi apparatus (53, 54) or from late endosomes to lysosomes (55, 56) also observed in some lysosomal storage diseases can produce similar accumulation. In chronic diseases, such ganglioside accumulation is typically detected in neurons (29, 30, 34, 57) and, in some cases, in activated microglia (51). However, neuronal accumulation of GM2

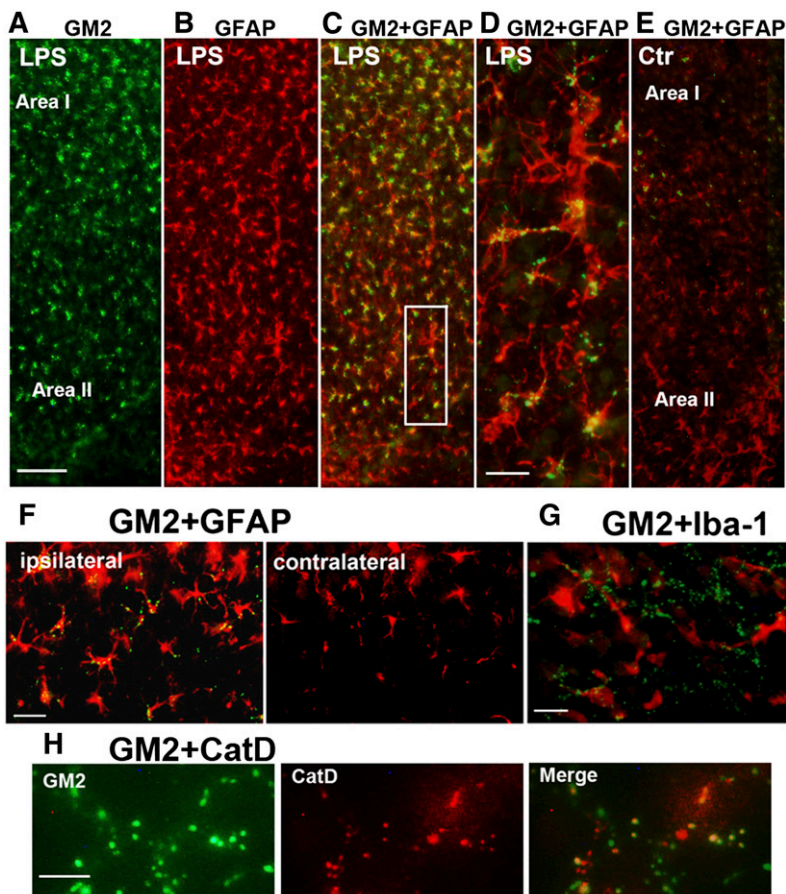


Fig. 9. LPS-induced GM2 accumulation in astrocytes. Twenty-four hours after injection of LPS intracerebrally into P7 C57BL/6By mice, brains were perfusion-fixed and the sections were dual-labeled with anti-GM2 (green) and anti-GFAP (red) (A–F), anti-GM2 (green) and anti-Iba-1 (red) (G), or anti-GM2 (green) and anti-CatD antibody (H). Panel (C) is a merged image of (A) and (B), and (D) is an enlarged image of the area of a square shown in (C). Panel (E) is a merged image (GM2 and GFAP) of a section from the control (saline-treated) brain, showing limited GM2 staining. LPS-induced GM2 elevation was observed mostly in the ipsilateral brain (F), and the presence of GM2 in microglia was scant (G), and some of the punctate GM2 staining was colocalized with CatD (H). The scale bar in (A) indicates 100  $\mu$ m, and the magnification of images of (B), (C), and (E) is the same as that of (A). Scale bars in (D), (F), and (G) indicate 20  $\mu$ m, and the scale bar in (H) indicates 5  $\mu$ m.



was relatively limited in our acute neonatal injury models (16), probably because of prompt clearance of apoptotic neurons generated acutely by ethanol (12).


Along with GM2 accumulation in microglia, ethanol-induced neurodegeneration in P7 WT mice was accompanied by appearance of GFAP<sup>+</sup>GM2<sup>+</sup> cells with the morphology of astrocytes. In agreement with previous studies (3), the number of GFAP<sup>+</sup> cells in the cortex increased 24 h after ethanol treatment, probably reflecting a reactive astrogliosis or enhancement of astrocyte differentiation. Intriguingly, many of these cells, especially in layer IV/V of the cortex (Area I) and the white matter area near the cingulum and external capsule (Area II), expressed punctate GM2 staining (Figs. 2, 6). Similar to the case with microglia, the appearance of GM2 in astrocytes arguably could originate from neuronal material or from intrinsic changes in ganglioside metabolism. The former is supported by evidence of GM2 colocalizing with lysosomal markers (LAMP1, CatD) (Fig. 2C) in astrocytes after ethanol exposure. This is compatible with degradation of phagocytosed material from degenerating neurons rich in gangliosides, and correlates with the rapid appearance of astrocytic GM2 in the deep cortical layers/corpus callosum area (Area II) where degenerating neurites are present (14) for potential engulfment. Phagocytosis by astrocytes has been documented in, for example, synaptic elimination during development (58) and elimination of dead cells following acute traumatic brain injury (59). The second explanation, astrocyte-intrinsic changes in gangliosides, is supported by the observed increase in GM2<sup>+</sup>GFAP<sup>+</sup> cells found with LPS treatment (Fig. 9) despite barely any evidence of neurodegeneration detectable by FJ staining, although LPS may induce degeneration of preoligodendrocytes, as reported in neonatal rats (40). Further investigation is needed to determine whether astrocyte activation/differentiation induced by ethanol or LPS increases *de novo* synthesis of GM2, but it has been shown that ethanol increases lipogenesis and *de novo* ceramide synthesis in the P7 brain (15, 17), and LPS induces augmentation of sphingolipid synthesis in the liver (60).

In adult rodents, GD3 increases in both activated microglia and reactive astrocytes (61). However, diffuse GD3 staining detected in neurons and glia in WT neonatal mice in this study was not significantly enhanced by ethanol treatment (data not shown). It could be that GFAP<sup>+</sup>GM2<sup>+</sup> cells only appear in the acutely injured developing brain. Interestingly, while after 24 h ethanol induced neurodegeneration and microglial activation in GalNAcT KO mice, they showed no significant increase in GFAP<sup>+</sup> cell number or GD3/GM3 in GFAP<sup>+</sup> cells. Pending time course studies to determine whether elevation in the GFAP<sup>+</sup> cell number might have been delayed or attenuated in KO mice, these results suggest that the loss of GM2/GD2 or other ganglioside series gangliosides in GalNAcT KO mice affects astrocyte activation/differentiation, while microglial activation is not deterred. Although the reason for this reduced astroglial activation in the KO mice remains to be clarified, there are several possibilities based on previous studies. First, it has been reported that both LPS and ethanol activate Toll-like

receptor 4 (TLR4) endocytosis and the subsequent signaling for inflammatory responses in cortical astrocytes, which are inhibited by the lipid raft disruption (62). Because lipid rafts of GalNAcT KO mice are partially disrupted because of the alteration in the ganglioside composition (63, 64), TLR4-mediated astrocyte activation may be disturbed in the KO mice. Further experiments involving TLR4 signaling, such as LPS treatment of the KO mice, may clarify this possibility. In this case, not only the lack of GM2, but also the lack of other downstream gangliosides, is likely to cause lipid raft disturbances (63, 64). Second, it is possible that a specific ganglioside (GM2, GD2, or other downstream gangliosides) is involved directly in acute astrocyte activation. Previous studies (65, 66) indicate that LacCer elevation is necessary for chronic pro-inflammatory activation of astrocytes. Likewise, GM2 or other downstream gangliosides may be necessary for acute astrocyte activation. Studies testing the effects of exogenous GM2 (or other gangliosides such as GM1) on ethanol/LPS-induced astrocyte activation in KO mice or in cultured astrocytes derived from KO mice may give insight into the roles of gangliosides in astrocyte activation.

Previously, we proposed that GM2 found in mitochondria in WT brain exposed to ethanol plays a role in neurodegenerative processes, because GM2, as well as GD3, enhanced cytochrome c release from isolated mitochondria (16, 21). The present experiments showing that ethanol still induced robust neurodegeneration in KO mice (Fig. 3) favor the putative importance of GD3 over GM2 in mitochondria-mediated apoptosis in GalNAcT KO mice, in line with a reported role for GD3 in CD95/Fas-mediated apoptosis in lymphocytes (21). It is also possible that the lack of neuroprotective GM1 ganglioside in KO mice rendered neurons more vulnerable to apoptotic stimuli, as shown in previous studies (67–69). While ethanol-induced microglial and astroglial activation observed in WT mice can be both beneficial and detrimental to neuronal degeneration (70–73), microglial phagocytosis is generally considered a neuroprotective process (74). Our previous and present studies indicate that activated microglia are engaged in the removal of dead neurons and thus help prevent further neurodegeneration (75, 76) without inducing classical neuroinflammation, as demonstrated in other binge ethanol exposure models in the developing (4) and adult brain (77). Considering that ethanol induced more neurodegeneration with less elevation in the number of GFAP<sup>+</sup> cells in GalNAcT KO mice, it is possible that GFAP<sup>+</sup>GM2<sup>+</sup> cells also exert neuroprotection rather than a deleterious neuroinflammation under our experimental conditions. It has been reported that hypoxic preconditioning of neonatal rats induces the precocious differentiation of astrocytes and exerts the neuroprotection (78). In this context, our preliminary studies indicate that LPS pretreatment in P7 mice attenuates or delays ethanol-induced neurodegeneration.

Thus, the present studies support our concept that GM2 elevation is associated with glial activation in the injured developing brain, and GM2 may be considered a sensitive marker for this pathological condition. Because GalNAcT

deletion alters the astroglial response during ethanol-induced neurodegeneration, GM2/GD2 or other downstream gangliosides may be involved in glial activation/differentiation. 

## REFERENCES

- Guerri, C., A. Bazinet, and E. P. Riley. 2009. Foetal alcohol spectrum disorders and alterations in brain and behaviour. *Alcohol Alcohol.* **44**: 108–114.
- Ikonomidou, C., P. Bittigau, M. J. Ishimaru, D. F. Wozniak, C. Koch, K. Genz, M. T. Price, V. Stefovskaja, F. Horster, T. Tenkova, et al. 2000. Ethanol-induced apoptotic neurodegeneration and fetal alcohol syndrome. *Science.* **287**: 1056–1060.
- Goodlett, C. R., J. T. Leo, J. P. O'Callaghan, J. C. Mahoney, and J. R. West. 1993. Transient cortical astrogliosis induced by alcohol exposure during the neonatal brain growth spurt in rats. *Brain Res. Dev. Brain Res.* **72**: 85–97.
- Kane, C. J., K. D. Phelan, L. Han, R. R. Smith, J. Xie, J. C. Douglas, and P. D. Drew. 2011. Protection of neurons and microglia against ethanol in a mouse model of fetal alcohol spectrum disorders by peroxisome proliferator-activated receptor-gamma agonists. *Brain Behav. Immun.* **25(Suppl 1)**: S137–S145.
- Kane, C. J., K. D. Phelan, and P. D. Drew. 2012. Neuroimmune mechanisms in fetal alcohol spectrum disorder. *Dev. Neurobiol.* **72**: 1302–1316.
- Tiwari, V., and K. Chopra. 2011. Resveratrol prevents alcohol-induced cognitive deficits and brain damage by blocking inflammatory signaling and cell death cascade in neonatal rat brain. *J. Neurochem.* **117**: 678–690.
- Ieraci, A., and D. G. Herrera. 2006. Nicotinamide protects against ethanol-induced apoptotic neurodegeneration in the developing mouse brain. *PLoS Med.* **3**: e101.
- Sadriani, B., S. Subbanna, D. A. Wilson, B. S. Basavarajappa, and M. Saito. 2012. Lithium prevents long-term neural and behavioral pathology induced by early alcohol exposure. *Neuroscience.* **206**: 122–135.
- Wilson, D. A., J. Peterson, B. S. Basavaraj, and M. Saito. 2011. Local and regional network function in behaviorally relevant cortical circuits of adult mice following postnatal alcohol exposure. *Alcohol. Clin. Exp. Res.* **35**: 1974–1984.
- Wozniak, D. F., R. E. Hartman, M. P. Boyle, S. K. Vogt, A. R. Brooks, T. Tenkova, C. Young, J. W. Olney, and L. J. Muglia. 2004. Apoptotic neurodegeneration induced by ethanol in neonatal mice is associated with profound learning/memory deficits in juveniles followed by progressive functional recovery in adults. *Neurobiol. Dis.* **17**: 403–414.
- Olney, J. W. 2002. New insights and new issues in developmental neurotoxicology. *Neurotoxicology.* **23**: 659–668.
- Olney, J. W., T. Tenkova, K. Dikranian, Y. Q. Qin, J. Labruyere, and C. Ikonomidou. 2002. Ethanol-induced apoptotic neurodegeneration in the developing C57BL/6 mouse brain. *Brain Res. Dev. Brain Res.* **133**: 115–126.
- Saito, M., R. F. Mao, R. Wang, C. Vadasz, and M. Saito. 2007. Effects of gangliosides on ethanol-induced neurodegeneration in the developing mouse brain. *Alcohol. Clin. Exp. Res.* **31**: 665–674.
- Saito, M., G. Chakraborty, R. F. Mao, S. M. Paik, C. Vadasz, and M. Saito. 2010. Tau phosphorylation and cleavage in ethanol-induced neurodegeneration in the developing mouse brain. *Neurochem. Res.* **35**: 651–659.
- Saito, M., G. Chakraborty, R. F. Mao, R. Wang, T. B. Cooper, C. Vadasz, and M. Saito. 2007. Ethanol alters lipid profiles and phosphorylation status of AMP-activated protein kinase in the neonatal mouse brain. *J. Neurochem.* **103**: 1208–1218.
- Saito, M., G. Chakraborty, R. Shah, R. F. Mao, A. Kumar, D. S. Yang, K. Dobrenis, and M. Saito. 2012. Elevation of GM2 ganglioside during ethanol-induced apoptotic neurodegeneration in the developing mouse brain. *J. Neurochem.* **121**: 649–661.
- Saito, M., G. Chakraborty, M. Hegde, J. Ohsie, S. M. Paik, C. Vadasz, and M. Saito. 2010. Involvement of ceramide in ethanol-induced apoptotic neurodegeneration in the neonatal mouse brain. *J. Neurochem.* **115**: 168–177.
- Saito, M., and M. Saito. 2013. Involvement of sphingolipids in ethanol neurotoxicity in the developing brain. *Brain Sci.* **3**: 670–703.
- Hakomori, S. 2003. Structure, organization, and function of glycosphingolipids in membrane. *Curr. Opin. Hematol.* **10**: 16–24.
- Ledeen, R. W., and G. Wu. 2002. Ganglioside function in calcium homeostasis and signaling. *Neurochem. Res.* **27**: 637–647.
- Malorni, W., A. M. Giammarioli, T. Garofalo, and M. Sorice. 2007. Dynamics of lipid raft components during lymphocyte apoptosis: the paradigmatic role of GD3. *Apoptosis.* **12**: 941–949.
- Zervas, M., and S. U. Walkley. 1999. Ferret pyramidal cell dendritogenesis: changes in morphology and ganglioside expression during cortical development. *J. Comp. Neurol.* **413**: 429–448.
- Constantopoulos, G., R. M. Eiben, and I. A. Schafer. 1978. Neurochemistry of the mucopolysaccharidoses: brain glycosaminoglycans, lipids and lysosomal enzymes in mucopolysaccharidosis type III B (alpha-N-acetylglucosaminidase deficiency). *J. Neurochem.* **31**: 1215–1222.
- Dawson, G., M. Fuller, K. M. Helmsley, and J. J. Hopwood. 2012. Abnormal gangliosides are localized in lipid rafts in Sanfilippo (MPS3a) mouse brain. *Neurochem. Res.* **37**: 1372–1380.
- McGlynn, R., K. Dobrenis, and S. U. Walkley. 2004. Differential subcellular localization of cholesterol, gangliosides, and glycosaminoglycans in murine models of mucopolysaccharide storage disorders. *J. Comp. Neurol.* **480**: 415–426.
- Micsenyi, M. C., K. Dobrenis, G. Stephney, J. Pickel, M. T. Vanier, S. A. Slaugenhaupt, and S. U. Walkley. 2009. Neuropathology of the Mcoln1(-/-) knockout mouse model of mucopolipidosis type IV. *J. Neuropathol. Exp. Neurol.* **68**: 125–135.
- Piccinini, M., F. Scandroglio, S. Prioni, B. Buccinna, N. Loberto, M. Aureli, V. Chigorno, E. Lupino, G. DeMarco, A. Lomartire, et al. 2010. Deregulated sphingolipid metabolism and membrane organization in neurodegenerative disorders. *Mol. Neurobiol.* **41**: 314–340.
- Wilkinson, F. L., R. J. Holley, K. J. Langford-Smith, S. Badrinath, A. Liao, A. Langford-Smith, J. D. Cooper, S. A. Jones, J. E. Wraith, R. F. Wynn, et al. 2012. Neuropathology in mouse models of mucopolysaccharidosis type I, IIIA and IIIB. *PLoS ONE.* **7**: e35787.
- Zervas, M., K. Dobrenis, and S. U. Walkley. 2001. Neurons in Niemann-Pick disease type C accumulate gangliosides as well as unesterified cholesterol and undergo dendritic and axonal alterations. *J. Neuropathol. Exp. Neurol.* **60**: 49–64.
- Zhou, S., C. Davidson, R. McGlynn, G. Stephney, K. Dobrenis, M. T. Vanier, and S. U. Walkley. 2011. Endosomal/lysosomal processing of gangliosides affects neuronal cholesterol sequestration in Niemann-Pick disease type C. *Am. J. Pathol.* **179**: 890–902.
- Barrier, L., S. Ingrand, M. Damjanac, A. Rioux Bilan, J. Hugon, and G. Page. 2007. Genotype-related changes of ganglioside composition in brain regions of transgenic mouse models of Alzheimer's disease. *Neurobiol. Aging.* **28**: 1863–1872.
- Kracun, I., S. Kalanj, J. Talan-Hranilovic, and C. Cosovic. 1992. Cortical distribution of gangliosides in Alzheimer's disease. *Neurochem. Int.* **20**: 433–438.
- Molander-Melin, M., K. Blennow, N. Bogdanovic, B. Dellheden, J. E. Mansson, and P. Fredman. 2005. Structural membrane alterations in Alzheimer brains found to be associated with regional disease development; increased density of gangliosides GM1 and GM2 and loss of cholesterol in detergent-resistant membrane domains. *J. Neurochem.* **92**: 171–182.
- Strømme, P., K. Dobrenis, R. V. Sillitoe, M. Gulinello, N. F. Ali, C. Davidson, M. C. Micsenyi, G. Stephney, L. Ellevog, A. Klungland, et al. 2011. X-linked Angelman-like syndrome caused by Slc9a6 knockout in mice exhibits evidence of endosomal-lysosomal dysfunction. *Brain.* **134**: 3369–3383.
- Woods, A. S., B. Colsch, S. N. Jackson, J. Post, K. Baldwin, A. Roux, B. Hoffer, B. M. Cox, M. Hoffer, V. Rubovitch, et al. 2013. Gangliosides and ceramides change in a mouse model of blast induced traumatic brain injury. *ACS Chem. Neurosci.* **4**: 594–600.
- Whitehead, S. N., K. H. Chan, S. Gangaraju, J. Slinn, J. Li, and S. T. Hou. 2011. Imaging mass spectrometry detection of gangliosides species in the mouse brain following transient focal cerebral ischemia and long-term recovery. *PLoS ONE.* **6**: e20808.
- Liu, Y., R. Wada, H. Kawai, K. Sango, C. Deng, T. Tai, M. P. McDonald, K. Araujo, J. N. Crawley, U. Bierfreund, et al. 1999. A genetic model of substrate deprivation therapy for a glycosphingolipid storage disorder. *J. Clin. Invest.* **103**: 497–505.
- Takamiya, K., A. Yamamoto, K. Furukawa, S. Yamashiro, M. Shin, M. Okada, S. Fukumoto, M. Haraguchi, N. Takeda, K. Fujimura, et al. 1996. Mice with disrupted GM2/GD2 synthase gene lack complex gangliosides but exhibit only subtle defects in their nervous system. *Proc. Natl. Acad. Sci. USA.* **93**: 10662–10667.



39. Hanslick, J. L., K. Lau, K. K. Noguchi, J. W. Olney, C. F. Zorumski, S. Mennerick, and N. B. Farber. 2009. Dimethyl sulfoxide (DMSO) produces widespread apoptosis in the developing central nervous system. *Neurobiol. Dis.* **34**: 1–10.
40. Cai, Z., Y. Pang, S. Lin, and P. G. Rhodes. 2003. Differential roles of tumor necrosis factor- $\alpha$  and interleukin-1  $\beta$  in lipopolysaccharide-induced brain injury in the neonatal rat. *Brain Res.* **975**: 37–47.
41. Matyash, V., G. Liebisch, T. V. Kurzchalia, A. Shevchenko, and D. Schwudke. 2008. Lipid extraction by methyl-tert-butyl ether for high-throughput lipidomics. *J. Lipid Res.* **49**: 1137–1146.
42. Ledeen, R. W., and R. K. Yu. 1982. Gangliosides: structure, isolation, and analysis. *Methods Enzymol.* **83**: 139–191.
43. Macala, L. J., R. K. Yu, and S. Ando. 1983. Analysis of brain lipids by high performance thin-layer chromatography and densitometry. *J. Lipid Res.* **24**: 1243–1250.
44. van Echten-Deckert, G. 2000. Sphingolipid extraction and analysis by thin-layer chromatography. *Methods Enzymol.* **312**: 64–79.
45. Paxinos, G., G. Halliday, C. Watspm, Y. Koutcherov, and H. Q. Wang. 2007. Atlas of the Developing Brain at E17.5, P0, and P6. Academic Press, Burlington, MA.
46. Furukawa, K., W. Aixinjueluo, T. Kasama, Y. Ohkawa, M. Yoshihara, Y. Ohmi, O. Tajima, A. Suzumura, D. Kittaka, and K. Furukawa. 2008. Disruption of GM2/GD2 synthase gene resulted in overt expression of 9-O-acetyl GD3 irrespective of Tis21. *J. Neurochem.* **105**: 1057–1066.
47. Saito, M., M. Saito, T. B. Cooper, and C. Vadasz. 2005. Ethanol-induced changes in the content of triglycerides, ceramides, and glucosylceramides in cultured neurons. *Alcohol. Clin. Exp. Res.* **29**: 1374–1383.
48. Chakraborty, G., M. Saito, R. F. Mao, R. Wang, C. Vadasz, and M. Saito. 2008. Lithium blocks ethanol-induced modulation of protein kinases in the developing brain. *Biochem. Biophys. Res. Commun.* **367**: 597–602.
49. Boche, D., V. H. Perry, and J. A. Nicoll. 2013. Review: activation patterns of microglia and their identification in the human brain. *Neuropathol. Appl. Neurobiol.* **39**: 3–18.
50. Hara, A., N. Kitazawa, and T. Taketomi. 1984. Abnormalities of glycosphingolipids in mucopolysaccharidosis type III B. *J. Lipid Res.* **25**: 175–184.
51. Ohmi, K., D. S. Greenberg, K. S. Rajavel, S. Ryazantsev, H. H. Li, and E. F. Neufeld. 2003. Activated microglia in cortex of mouse models of mucopolysaccharidoses I and IIIB. *Proc. Natl. Acad. Sci. USA.* **100**: 1902–1907.
52. Kolter, T., and K. Sandhoff. 2010. Lysosomal degradation of membrane lipids. *FEBS Lett.* **584**: 1700–1712.
53. Marks, D. L., and R. E. Pagano. 2002. Endocytosis and sorting of glycosphingolipids in sphingolipid storage disease. *Trends Cell Biol.* **12**: 605–613.
54. Vitner, E. B., F. M. Platt, and A. H. Futerman. 2010. Common and uncommon pathogenic cascades in lysosomal storage diseases. *J. Biol. Chem.* **285**: 20423–20427.
55. Lloyd-Evans, E., H. Waller-Evans, K. Peterneva, and F. M. Platt. 2010. Endolysosomal calcium regulation and disease. *Biochem. Soc. Trans.* **38**: 1458–1464.
56. Tancini, B., A. Magini, L. Latterini, L. Urbanelli, V. Ciccarone, F. Elisei, and C. Emiliani. 2010. Occurrence of an anomalous endocytic compartment in fibroblasts from Sandhoff disease patients. *Mol. Cell. Biochem.* **335**: 273–282.
57. Liu, Y., Y. P. Wu, R. Wada, E. B. Neufeld, K. A. Mullin, A. C. Howard, P. G. Pentchev, M. T. Vanier, K. Suzuki, and R. L. Proia. 2000. Alleviation of neuronal ganglioside storage does not improve the clinical course of the Niemann-Pick C disease mouse. *Hum. Mol. Genet.* **9**: 1087–1092.
58. Chung, W. S., L. E. Clarke, G. X. Wang, B. K. Stafford, A. Sher, C. Chakraborty, J. Joung, L. C. Foo, A. Thompson, C. Chen, et al. 2013. Astrocytes mediate synapse elimination through MEGF10 and MERTK pathways. *Nature.* **504**: 394–400.
59. Lööf, C., L. Hillered, T. Ebendal, and A. Erlandsson. 2012. Engulfing astrocytes protect neurons from contact-induced apoptosis following injury. *PLoS ONE.* **7**: e33090.
60. Memon, R. A., W. M. Holleran, Y. Uchida, A. H. Moser, S. Ichikawa, Y. Hirabayashi, C. Grunfeld, and K. R. Feingold. 1999. Regulation of glycosphingolipid metabolism in liver during the acute phase response. *J. Biol. Chem.* **274**: 19707–19713.
61. Amat, J. A., H. Ishiguro, K. Nakamura, and W. T. Norton. 1996. Phenotypic diversity and kinetics of proliferating microglia and astrocytes following cortical stab wounds. *Glia.* **16**: 368–382.
62. Pascual-Lucas, M., S. Fernandez-Lizarbe, J. Montesinos, and C. Guerri. 2014. LPS or ethanol triggers clathrin- and rafts/caveolae-dependent endocytosis of TLR4 in cortical astrocytes. *J. Neurochem.* **129**: 448–462.
63. Ohmi, Y., O. Tajima, Y. Ohkawa, Y. Yamauchi, Y. Sugiura, K. Furukawa, and K. Furukawa. 2011. Gangliosides are essential in the protection of inflammation and neurodegeneration via maintenance of lipid rafts: elucidation by a series of ganglioside-deficient mutant mice. *J. Neurochem.* **116**: 926–935.
64. Ohmi, Y., Y. Ohkawa, Y. Yamauchi, O. Tajima, K. Furukawa, and K. Furukawa. 2012. Essential roles of gangliosides in the formation and maintenance of membrane microdomains in brain tissues. *Neurochem. Res.* **37**: 1185–1191.
65. Mayo, L., S. A. Trauger, M. Blain, M. Nadeau, B. Patel, J. I. Alvarez, I. D. Mascanfroni, A. Yeste, P. Kivisakk, K. Kallas, et al. 2014. Regulation of astrocyte activation by glycolipids drives chronic CNS inflammation. *Nat. Med.* **20**: 1147–1156.
66. Pannu, R., J. S. Won, M. Khan, A. K. Singh, and I. Singh. 2004. A novel role of lactosylceramide in the regulation of lipopolysaccharide/interferon- $\gamma$ -mediated inducible nitric oxide synthase gene expression: Implications for neuroinflammatory diseases. *J. Neurosci.* **24**: 5942–5954.
67. Wu, G., Z. H. Lu, X. Xie, and R. W. Ledeen. 2004. Susceptibility of cerebellar granule neurons from GM2/GD2 synthase-null mice to apoptosis induced by glutamate excitotoxicity and elevated KCl: rescue by GM1 and LIGA20. *Glycoconj. J.* **21**: 305–313.
68. Wu, G., Z. H. Lu, J. Wang, Y. Wang, X. Xie, M. F. Meyenhofer, and R. W. Ledeen. 2005. Enhanced susceptibility to kainate-induced seizures, neuronal apoptosis, and death in mice lacking gangliotetraose gangliosides: protection with LIGA 20, a membrane-permeant analog of GM1. *J. Neurosci.* **25**: 11014–11022.
69. Wu, G., Z. H. Lu, N. Kulkarni, R. Amin, and R. W. Ledeen. 2011. Mice lacking major brain gangliosides develop parkinsonism. *Neurochem. Res.* **36**: 1706–1714.
70. Boyadjieva, N. I., and D. K. Sarkar. 2013. Microglia play a role in ethanol-induced oxidative stress and apoptosis in developing hypothalamic neurons. *Alcohol. Clin. Exp. Res.* **37**: 252–262.
71. Crews, F. T., and K. Nixon. 2009. Mechanisms of neurodegeneration and regeneration in alcoholism. *Alcohol Alcohol.* **44**: 115–127.
72. Dheen, S. T., C. Kaur, and E. A. Ling. 2007. Microglial activation and its implications in the brain diseases. *Curr. Med. Chem.* **14**: 1189–1197.
73. Neher, J. J., U. Nenislyte, J. W. Zhao, A. Bal-Price, A. M. Tolkovsky, and G. C. Brown. 2011. Inhibition of microglial phagocytosis is sufficient to prevent inflammatory neuronal death. *J. Immunol.* **186**: 4973–4983.
74. Sierra, A., O. Abiega, A. Shahraz, and H. Neumann. 2013. Janus-faced microglia: beneficial and detrimental consequences of microglial phagocytosis. *Front. Cell. Neurosci.* **7**: 6.
75. Elliott, M. R., and K. S. Ravichandran. 2010. Clearance of apoptotic cells: implications in health and disease. *J. Cell Biol.* **189**: 1059–1070.
76. Sokolowski, J. D., and J. W. Mandell. 2011. Phagocytic clearance in neurodegeneration. *Am. J. Pathol.* **178**: 1416–1428.
77. Marshall, S. A., J. A. McClain, M. L. Kelso, D. M. Hopkins, J. R. Pauly, and K. Nixon. 2013. Microglial activation is not equivalent to neuroinflammation in alcohol-induced neurodegeneration: The importance of microglia phenotype. *Neurobiol. Dis.* **54**: 239–251.
78. Sen, E., A. Basu, L. B. Willing, T. F. Uliasz, J. L. Myrkal, S. J. Vannucci, S. J. Hewett, and S. W. Levison. 2011. Pre-conditioning induces the precocious differentiation of neonatal astrocytes to enhance their neuroprotective properties. *ASN Neuro.* **3**: e00062.
79. Svennerholm, L. 1963. Chromatographic separation of human brain gangliosides. *J. Neurochem.* **10**: 613–623.